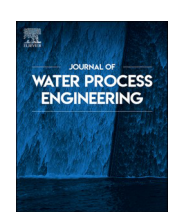
ELSEVIER

Contents lists available at ScienceDirect

## Journal of Water Process Engineering

journal homepage: www.elsevier.com/locate/jwpe





# Continuous electrocoagulation-membrane distillation unit for treating hydraulic fracturing produced water

Yuhe Cao <sup>a,\*</sup>, Mahdi Malmali <sup>b</sup>, Xianghong Qian <sup>c</sup>, S. Ranil Wickramasinghe <sup>a,d,\*</sup>

- <sup>a</sup> Ralph E Martin Department of Chemical Engineering, University of Arkansas, Fayetteville, AR 72701, United States
- <sup>b</sup> Department of Chemical Engineering, Texas Tech University, Lubbock, TX 79409, United States
- <sup>c</sup> Department of Biomedical Engineering, University of Arkansas, Fayetteville, AR 72701, United States
- d Department of Civil & Environmental Engineering, Technion—Israel Institute of Technology, Haifa 32000, Israel

#### ARTICLE INFO

# Keywords: Oily water Electrocoagulation Sludge Wastewater Water recovery Water treatment

#### ABSTRACT

Hydraulic fracturing oil and gas produced water is frequently highly impaired. While it is often deep well injected, there is great interest in treating this water for beneficial uses. Given the complexity of these produced waters, multiple unit operations are necessary. Electrocoagulation has been considered as a promising pretreatment technology. Here electrocoagulation is considered as a pretreatment prior to membrane distillation. The focus of this work is on understanding the electrocoagulation process in order to design an integrated unit operation. Electrocoagulation is used to remove organic compounds that will foul the membrane leading to membrane failure during membrane distillation. Using aluminum or iron electrodes, half-cell reactions in the electrocoagulation cell and electrode potentials have been calculated. Electrocoagulation was conducted using a continuous electrocoagulation reactor with actual produced water using aluminum, iron or mixed aluminum and iron electrodes. The results obtained here indicate that electrocoagulation can obtain good removal efficiency of total organic carbon (TOC) by using different reaction conditions. Removal of organic compounds is essential to minimize fouling during membrane distillation. Further the performance of the electrocoagulation process depends strongly on the quality of the feed water. Insoluble species were more effectively coagulated than dissolved organic species. Continuous electrocoagulation shows great potential as a scalable unit operation for pretreating hydraulic fracturing produced water.

## 1. Introduction

Sustainable water management practices will require maximizing water recovery, recycle, and reuse [1]. Co-produced water is the largest waste stream from oil and gas production [2–4]. Here the focus is on hydraulic fracturing operations. Hydraulic fracturing technology has enabled the recovery of oil and gas from low-permeability rocks such as tight sandstone, shale and coal beds [5,6]. Hydraulic fracturing operations involve injecting water and proppant (ceramic or sand) containing about 2 % added fracturing fluid (frac fluid) under pressure into the rock formation [7]. Frac fluids consist of additives such as biocides, scale inhibitors, solvents, friction reducers, corrosion inhibitors and non-ionic surfactants [7–9]. The high pressure liquid is used to fracture the rock formation. The pressure is released and the flow back water plus oil or gas and co-produced water is recovered. The proppant used in hydraulic fracturing prevents collapse of the fissures created in the rock formation.

Thus, the permeability of the rock is increased allowing recovery of the oil or gas.

Disposal of flow back and co-produced water, referred to as produced water, is a major environmental challenge [10,11]. Due to the added frac fluid, oil, and contaminants from the geological formation, it is highly impaired. Frequently multiple unit operations are needed if the water is to be treated and reused for beneficial applications. The level of treatment of the produced water depends on the beneficial use of the treated water [9,12–15].

The first stage of treatment, primary treatment, is sufficient to remove suspended solids and free oil from the produced water resulting in water for deep well injection into a geologically isolated formation. Secondary treatment is used to further treat the water for reuse to stimulate new wells. Finally, tertiary treatment operations result in water which can be discharged directly into lakes and rivers. Jiménez et al. provide a detailed summary of the unit operations typically considered for primary, secondary, and tertiary treatment of produced

<sup>\*</sup> Corresponding authors at: Ralph E. Martin Department of Chemical Engineering, University of Arkansas, Fayetteville, AR, USA. *E-mail addresses*: caoyh618@hotmail.com (Y. Cao), swickram@uark.edu (S.R. Wickramasinghe).

Nomenclature		
BPS	Bipolar Series	
C/F	Carbon/Fluorine	
DI	Deionized	
E	Redox Potentials	
EC	Electrocoagulation	
Н	Height of the Liquid-sludge Interface at Time t	
LSCM	Laser Scanning Confocal Microscopy	
MD	Membrane Distillation	
O/F	Oxygen/Fluorine	
SEM	Scanning Electron Microscopy	
SVI	Sludge Volume Index	
TDS	Total Dissolved Solids	
TOC	Total Organic Carbon	
TSS	Total Suspended Solids	

#### water [3].

Here an electrocoagulation (EC) process has been developed for pretreating produced water prior to membrane distillation. While previous investigators have tended to focus on optimizing the membrane distillation operation, this paper focus on understanding the EC process thus providing new insights into the development of a combined unit operation. Several advantages can be achieved when using EC compared to chemical coagulation, such as elimination of flocculant addition, ease of operation, production of more easily separable flocs, lower sludge volume, and efficient removal of the smallest colloidal particles [16-21]. EC has been used as a pretreatment process or a post-treatment process depending on the type of wastewater, showing that it is effective at removing contaminants when integrated with other treatment methods [22-26]. In EC ions are supplied by a sacrificial electrode. However, depending on the electrode potential, direct reaction with species in the water can occur on the electrode surface. Charged species in the wastewater are removed by reaction with oppositely charged ions or with flocs of metallic hydroxide generated in the wastewater [27]. The performance of membrane distillation is compared with and without pretreatment by EC.

## 2. Theoretical background

## 2.1. Half-cell reactions and electrode potentials

EC is a complex process involving electrochemical metal dissolution while water is reduced. Some of the pollutants present could be oxidized or reduced. In addition, chemical reactions such as acid/base reactions with pH changes, hydroxide precipitation, redox reaction in the bulk solution, as well as physical processes such as adsorption and coagulation occur. The EC process begins with dissolution of a sacrificial electrode. Table 1 gives the standard state reduction potentials [28] at 25 °C for possible reactions that may occur during EC of the produced water samples tested here. At the anode, the metal present in the sacrificial metal electrode is oxidized.

$$M \rightarrow M^{z+} + ze^{-} \tag{1}$$

where M is the metal atom and z is the number of electrons transferred per metal atom [29]. If a high anode potential is used (large voltage differences between the anode and cathode), secondary reactions such as the oxidation of water can occur [30,31] leading to a local decrease in pH and oxygen generation. Similarly in the presence of  $Cl^-$  ions,  $Cl_2$  could be produced. At the cathode reduction of water occurs. (see Table 1).

$$2H_2O + 2e \to H_2 + 2OH^- \tag{2}$$

It is important to note that Faraday's law only applies when all the electrons in the system participate in the metal dissolution reaction. When competing reactions occur a current efficiency factor must be used. In the case of a sacrificial Al electrode, the reduction potential of  $\mathrm{Al}^{3+}$  is lower than that of water (see Table 1). Consequently, both chemical and electrochemical dissolution are possible. In fact, Cañizares et al. indicate that the two processes often occur in parallel which could lead to a current efficiency greater than 1 [32]. Given the complexity of produced water and the presence of many other species other side reactions are also possible.

Variations from standard conditions may be accounted for using the Nernst equation, [33]:

$$E = E^{\circ} - \left(\frac{2.303RT}{nF}\right) log\left(\prod [product]^{X} / \prod [reactants]^{Y}\right)$$
 (15)

where  $R = 8.314 \text{ J mol}^{-1} \text{ K}^{-1}$ , T = 298 K,  $F = 96,490 \text{ C mol}^{-1}$ , n = mole of electrons involved in the reaction. The superscripts x and y are the stoichiometric coefficients of the products in the half cell equation. Substituting for the constants into the above equation yields the following:

$$E = E^{\circ} - \left(\frac{0.0591}{n}\right) log\left(\prod [product]^{X} / \prod [reactants]^{Y}\right)$$
 (16)

For the produced water investigated here (see Table 2), pH = 7.2 and [Cl $^-$ ] = 89,266.0 mg L $^{-1}$  = 2.51 M. The reduction potentials were then calculated using the Nernst Equation and E-pH diagram [29]. Fig. 1 shows the reduction potentials for species transformation using the produced water as the electrolyte solution.

Having been released from the anode, the metal ions usually form metal hydroxides that have low solubility and can precipitate. However specially for aluminum ions, various equilibrium acid/base, complexation, precipitation, and redox reactions occur. Water soluble pollutants typically organic species, in the produced water adsorb onto the precipitates. Colloidal suspensions are destabilized during EC. Coagulation of these particles occurs due to interactions between the soluble ions generated by metal dissolution from the sacrificial electrodes. This leads to a reduction in the repulsive forces between particles resulting in aggregation [29].

Charge neutralization by adsorption of metal ion species will also lead to aggregation. Finally, entrapment of colloidal particles within a hydroxide precipitate will lead to aggregation. The destabilization processes occur in parallel. The extent to which any one process dominates depends on the prevailing conditions. After destabilization, floculation occurs, the rate of which depends on the degree of destabilization of the colloidal particles as well as the particle collision rate. The flocs can rise due to the rising hydrogen gas produced. The flocs eventually age, densify and settle to the bottom. The flocculated material or sludge can be removed by sedimentation. Here, after sludge removal the treated water is further processed by direct contact

**Table 1**Standard reduction potentials at 25 °C.

Half-reaction	E° (V)
$H_2O_2(aq) + 2H^+(aq) + 2e^- \rightarrow 2H_2O$ (3)	+1.77
$Cl_2(g) + 2e^- \rightarrow 2Cl^-(aq)$ (4)	+1.36
$O_2(g) + 4H^+(aq) + 2e^- \rightarrow 2H_2O$ (5)	+1.23
$Fe^{3+}(aq) + e^{-} \rightarrow Fe^{2+}(aq)$ (6)	+0.77
$O_2(g) + 2H^+(aq) + 2e^- \rightarrow H_2O_2(aq)$ (7)	+0.68
$O_2(g) + 2H_2O + 4e^- \rightarrow 4OH^-(aq)$ (8)	+0.40
$2H^+(aq) + 2e^- \to H_2(g)$ (9)	0.00
$Fe^{2+}(aq) + 2e^{-} \rightarrow Fe(s)$ (10)	-0.44
$2H_2O + 2e^- \rightarrow H_2(g) + 2OH^-(aq)$ (11)	-0.83
$Al^{3+}(aq) + 3e^{-} \rightarrow Al(s)$ (12)	-1.66
$Mg^{2+}(aq) + 2e^{-} \rightarrow Mg(s)$ (13)	-2.37
$Ca^{2+}(aq) + 2e^{-} \rightarrow Ca(s)$ (14)	-2.87

**Table 2** Characterization of produced water.

Parameter	Produced water	Unit
TDS	134,787.1	${\rm mg~L^{-1}}$
TOC	157	${ m mg~L}^{-1}$
TSS	38.2	${ m mg~L}^{-1}$
Turbidity	16.5	NTU's
pH	7.2	-
Chloride	89,266.0	${\sf mg}\ {\sf L}^{-1}$
Nitrate	0.611	${\sf mg}\ {\sf L}^{-1}$
Sulfate	758.1	${\sf mg}\ {\sf L}^{-1}$
Aluminum	0	${\sf mg}\ {\sf L}^{-1}$
Iron	0.005	${\sf mg}\ {\sf L}^{-1}$
Boron	_	${\sf mg}\ {\sf L}^{-1}$
Calcium	3,718.9	${ m mg~L^{-1}}$
Strontium	352	${ m mg~L^{-1}}$
Magnesium	677.3	${\sf mg}\ {\sf L}^{-1}$
Manganese	0.193	${\sf mg}\ {\sf L}^{-1}$
Nickel	_	${\sf mg}\ {\sf L}^{-1}$
Potassium	1,036.24	${\sf mg}\ {\sf L}^{-1}$
Sodium	57,273.0	${\sf mg}\ {\sf L}^{-1}$
Conductivity	181,900	μS/cm
Total nitrogen	79.14	${ m mg~L^{-1}}$

## membrane distillation [25].

In the EC process investigated here, both the cathode and anode consisted of either iron or aluminum. In addition, a mixed electrode set up was used where the bipolar electrodes were iron and aluminum but the anode and cathode at the end of the array of electrodes were the same (iron electrodes). Other variations have been proposed where changes are made to the cathode material or the solution [34–36].

#### 3. Materials and methods

## 3.1. Materials

The produced water was collected from the oil fields in Texas, USA. It was treated with  $\text{ClO}_2$  at the oil field. It is common that produced water is treated by  $\text{ClO}_2$  is to reduce emulsion formation due to iron and to control microbial growth. The produced water was analyzed by the Arkansas Water Resources Center, University of Arkansas (Fayetteville, AR, USA). Deionized (DI) water used throughout the investigation was collected from Thermo Fisher 18 M $\Omega$  Barnstead Smart2Pure system (Schwerte, Germany). Deionized water was used for rinsing and washing the electrodes and other equipment. Aluminum and alloy steel sheets with thickness of 0.04" were purchased from OnlineMetals.com (Seattle, WA).

## 3.2. EC reactor design and operation

Three electrode configurations were considered: 5 iron; 3 iron and 2 aluminum and 5 aluminum. Each electrode configuration was tested using current of 3 A and 5 A for 5 min. The 5 min reaction time was based on our previous results, which indicate this as an appropriate reaction time. Similarly 3 and 5 A were chosen based on previous work. Longer reaction times and higher currents may not be practical. Shorter reaction times generally do not lead to addition of sufficient ions [37]. A DC power supply (Hewlett Packard, Palp Alto, CA) was used with cathode and anode attached to electrodes with a bipolar series (BPS) electrode arrangement (only the first and last electrodes are connected directly to the power supply). Hakizimana et al. [29] and Garcia-Sergura et al. [38] provide a summary of the various electrode arrangements that are commonly used and their advantages and disadvantages. The formation of passivation layers on the electrodes was mitigated by a reverse polarity switch connected directly to the DC power to enable the direction of the current to alternate every 30 s. These passivation layers can suppress further reactions if reverse polarity were not used [39,40]. Before each experiment, the electrodes were cleaned (using 10 % (v/v)

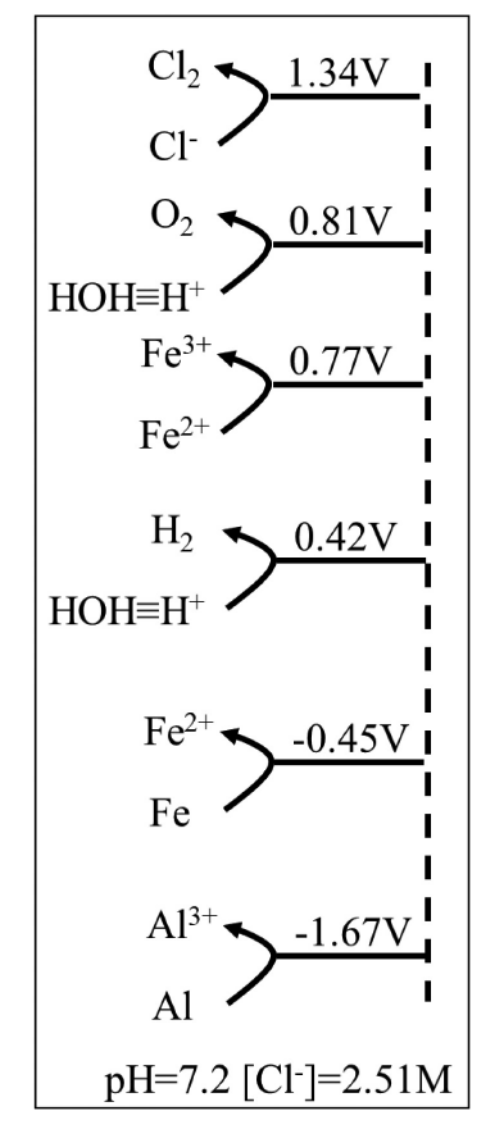


**Fig. 1.** Redox potentials (E) for half reactions that can occur on the Fe or Al anode surface during EC. The redox potential is reported for produced water (pH = 7.2, [Cl $^-$ ] = 2.51 M), and other parameters are considered at standard state conditions.

nitric acid solution), sandpapered, and dried.

Fig. S1 (supplementary data) is a schematic diagram of the continuous EC reactor. A custom-built polycarbonate EC reactor with a total volume of 1078 cm³ was used to conduct all the EC experiments. There are two chambers in the reactor, the left one is the main reaction chamber having dimensions of 7 cm  $\times$  11 cm  $\times$  14 cm, which holds the electrodes. The right one is an overflow chamber that collects the treated water from outlet 4, see Fig. S1A. The inlet to the reactor is connected with a liquid distributor with many holes to disperse the feed water evenly, see Fig. S1B. Five electrodes were fitted vertically inside the reactor with a 10 mm inter electrode spacing and an effective surface area of 770 cm². Based on earlier screening studies a constant current of 3 or 5 A was tested here. A constant current was maintained resulting in a variation in voltage across the electrodes due to changes in conductivity of the produced water during electrocoagulation.

As shown in Fig. S2 (supplementary data), 3 L of produced water were pumped into the reactor. Tracer tests using a dye solution were conducted to ensure dead zones were minimized. In order to prevent the formation of dead zones the reactor contents were stirred. Fig. S3B (supplementary data) shows the spreading of the dye solution at low

flow rate (0.2 L/min) in the presence of mixing. As can be seen no dead zone can be observed. Consequently, stirring was included. The detailed configuration of the electrodes in the reactor is illustrated in Fig. S4 (supplementary data).

## 3.3. Sludge settling test

In all EC experiments, the first liter of treated water was wasted to ensure steady state was reached. This was verified by making sure the current was stabilized, which usually takes about 30 s. Then, treated water, approximately 1 L of water, was collected using the second liter from the feed tank. This sample was allowed to sediment and the supernatant used for membrane distillation (MD).

Sludge settling tests were conducted using 1 L graduated cylinder. The height of the liquid-sludge interface (H) was recorded periodically over 3 h. The dimensionless height of the liquid-sludge interface is  $\rm H/H_0$  (height of the liquid-sludge interface at time t/initial height of the EC treated water). We note that the flocs initially rise due to production of hydrogen generated even after the water has been removed from the EC cell.

### 3.4. MD

To investigate the effect of EC on MD performance, EC pretreated, and non-pretreated water was tested. The MD system used here has been described in our previous work [25], which is shown in Fig. 2. A custom-made acrylic membrane cell with 40 cm<sup>2</sup> effective membrane area and 2 mm deep channels was used as the membrane module. PTFE spacers (ET 8700, Industrial Netting, Minneapolis, MN, USA) were used for mechanical support and mixing.

Feed and permeate streams were pumped on opposite sides of the membrane in counter current flow (at 0.5 L/min) using two peristaltic pumps (Masterflex I/P, Cole Parmer, Vernon Hills, IL). The weight of the permeate was measured and recorded by a computer-connected analytical balance (Mettler Toledo, Columbus, OH, USA). The feed water was maintained at 60  $^{\circ}\text{C}$  by a heat exchanger (heated by the circulating oil from a heater (PolyScience, Niles, IL, USA)). The temperature of the permeate tank was maintained at 20  $^{\circ}\text{C}$  using an external chiller (PolyScience, Niles, IL, USA). The water flux was calculated based on the weight change of the permeate tank. The permeate conductivity was continuously monitored using a conductivity meter (VWR, Radnor, PA, USA).

MD experiments were run with an initial produced water feed volume of 800 mL. DI water was added to replace the permeate that was removed during the run. The experiment was run for 6 h. After this, additional 200 mL of the same original feed produced water was added to the feed tank and the feed and permeate were removed without replacement. Consequently, the contents of the feed tank were

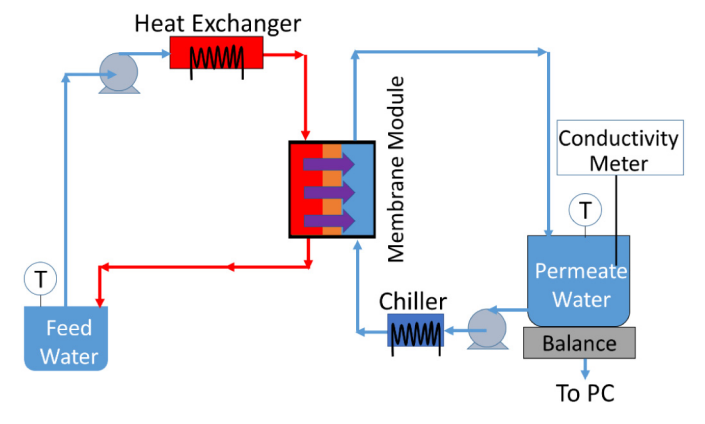


Fig. 2. Diagram of MD system investigated here [25].

concentrated.

### 3.5. Material characterization

## 3.5.1. Produced water characterization

A Shimadzu TOC-Vcsh (Shimadzu scientific instruments, Colombia, MD) was used to measure the total organic carbon (TOC) using EPA standard method 180.1. EPA standard methods 160.1, 160.2, and 415.1 were used to measure total dissolved solid (TDS), total suspended solids (TSS), and turbidity, respectively. A conductivity meter (VWR, Radnor, PA) was used to measure the conductivity. Finally, the cations and anions measured here were according to EPA methods 200.7 and 300.0, respectively.

## 3.5.2. Sludge and membrane characterization

Scanning electron microscopy (SEM) was used to determine the surface morphology and elemental analysis, for each membrane before and after MD using Nova Nanolab 200 Duo-Beam Workstation (FEI, Hillsboro, OR USA). To further compare the difference between the iron hydroxide flocs and aluminum hydroxide flocs, LS 13320 Particle Size Analyzer (Beckman Coulter, Brea, CA, USA), SEM and laser scanning confocal microscopy (LSCM) (Leica SP5 confocal microscopes, Leica Microsystems, Buffalo Grove, IL, USA) were employed to investigate their morphology and physical characteristics.

## 4. Results and discussion

## 4.1. Sludge settling characterization

Results for the analysis of the produced water used here are given in Table 2. As can be seen the water is highly impaired as the TDS, TOC, TSS, and turbidity are all very high. The main inorganic ions present are sodium, potassium, calcium and chloride.

A solid-liquid interface was visible after the EC treated water was placed in the graduated cylinder. The dimensionless height of the solid-liquid interface versus the settling time for different electrode configurations is illustrated in Fig. 3A and B. As can be seen for the higher current, 5 A, using only Al electrodes, there is an initial short period of relatively slow sludge settling followed by an increased rate of settling. This is most likely due to the formation of a gel of polymeric hydroxides [41] This period of initial slow settling is significantly reduced for a current of 3 A and the subsequent decrease in the solid liquid interface height is much faster. This is due to the lower number of Al ions that are released.

The settling curves for iron and iron/aluminum electrode combinations are quite different. Iron ions do not form polymeric hydroxides analogous to aluminum [41]. There is no visible initial slow settling period. Rather a much more rapid decrease in the solid liquid interface occurs very quickly known as the regime of zone settling [42–44]. Next a slower transition settling region is reached. Finally, compression settling is the last settling period with a steady and much smaller rate of height decrease of the solid-liquid interface. For the effluent treated by iron electrodes at same operating conditions, more rapid settling was observed than with aluminum electrodes.

This experimental observation can be interpreted as follows. At a higher current density, the extent of anodic metal dissolution increases, resulting in a greater amount of precipitate [41]. The solids concentration increases but the settling resistance also increases, which decreases the sludge settling velocity. This is particularly true for polymeric aluminum hydroxides. In addition, unlike iron hydroxides, higher concentration of aluminum hydroxide may result in significant gel formation.

## 4.2. Sludge volume index

Sludge volume index (SVI) is frequently used to characterize settle-

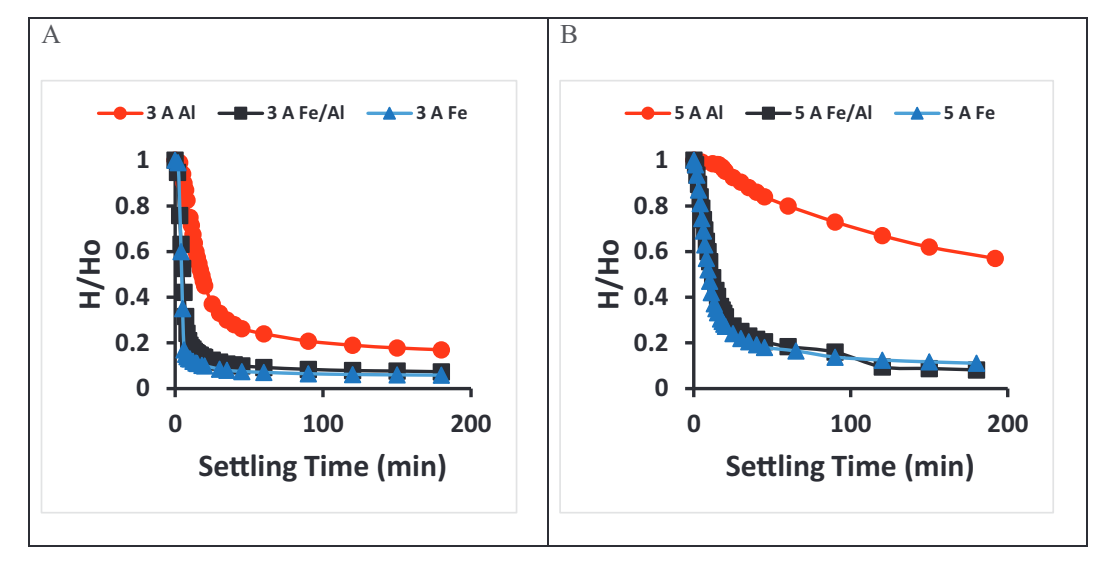


Fig. 3. Effect of different electrodes arrangements on the dimensionless height of solid-liquid interface using applied current of: A) 3 A; B) 5 A.

ability. It is the dimensionless sludge height after 30 min of settling normalized by the initial sludge concentration.

$$SVI = \frac{H_{30}}{H_0 \ x \ SS} 1000 \ (mL \ L^{-1})$$

where  $H_{30}$  is the sludge height after 30 min settling (cm),  $H_0$  is the initial height of the sludge after EC in the settling column (cm) and SS is the initial sludge concentration after EC (g L<sup>-1</sup>). Results are given in Fig. 4.

A higher SVI indicates poorer compressibility of the sludge [45,46]. The results indicate that higher currents give a less compressible sludge [47]. The SVI for aluminum electrodes (525.3 mL/g) is higher than the Fe electrodes (100.2 mL/g) at 3A. It is apparent that the SVI for mixed electrodes is between the Al and Fe electrodes. Since the SVI is related to the change in the height of the solid liquid interface during settling, the results in Figs. 3 and 4 are in agreement.

## 4.3. TOC removal

Fig. 5 indicates that TOC removal is improved at 5A compared to 3A for both aluminum and iron electrodes. For mixed iron/aluminum electrodes there is no difference in TOC removal at higher current. However as shown in Fig. 4 the sludge volume index increased at a higher current for mixed iron and aluminum electrodes. Therefore, it is essential to consider having not only high TOC removal but also flocs that settled (low SVI) easily when evaluating the EC operating conditions.

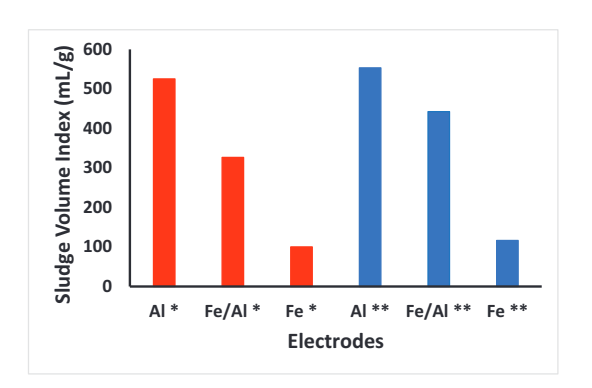


Fig. 4. SVI for the different experimental conditions. Note: \* is 3 A and \*\* is 5 A.

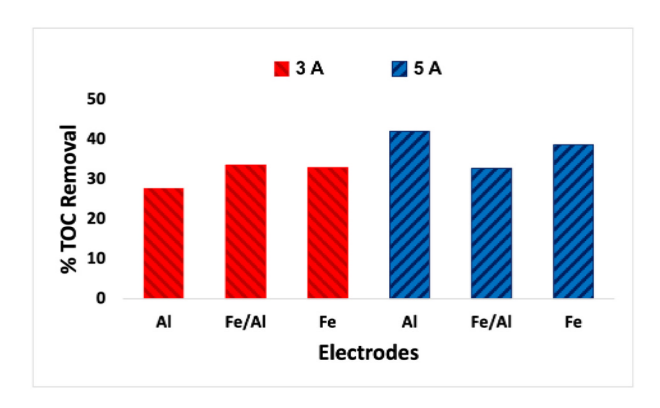
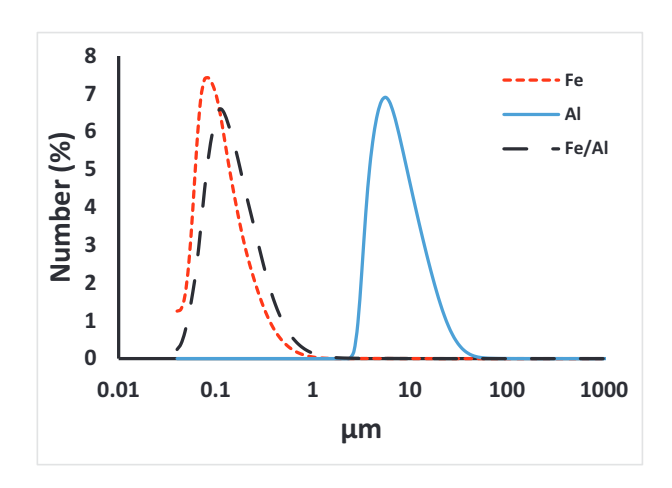


Fig. 5. TOC removal under different conditions. Note: the TOC of produced water was  $157~\mathrm{ppm}$ .

## 4.4. Sludge characterization

Fig. 6 gives particle size distribution for the various flocs generated under the EC conditions of 5 A current and 5 min reaction time after settling for 3 h. The number distribution (Fig. 6) indicates the Al flocs are large than the Fe and Fe Al flocs at 5 A current. Floc morphology was



**Fig. 6.** Particle size distribution for different electrode combinations at 5 A: particle size versus number percentage.

investigated by LSCM. The results are given in Fig. 7. As can be seen, the aluminum flocs are longer compared to the iron hydroxide flocs. The flocs from the hybrid electrodes have both long-entangled pieces and irregular sphere. The  ${\rm Al}^{3+}$  and  ${\rm OH}^-$  generated at the electrodes react to form various monomeric and polymeric aluminum hydroxide species, such as  ${\rm Al(OH)}^{2+}$ ,  ${\rm Al_6(OH)}^{3+}_{15}$ ,  ${\rm Al_7(OH)}^{4+}_{17}$  and  ${\rm Al_{13}(OH)}^{3+}_{34}$ , which undergo complex polymerization and partly transform into insoluble amorphous aluminum hydroxides according to complex precipitation kinetics [32,48,49]. These precipitates act as "swift flocs" and form long pieces with an open structure and have large surface areas which are helpful for fast adsorption of contaminants from wastewater [50].

Note: A, B, and C are images at 200 times magnification; D, E, and F are images at 400 times magnification.

The floc morphology was further investigated by filtering the sludge with filter paper and drying it. Sludges produced for a current of 5 A using different electrode configurations were investigated. These dried sludge samples were characterized by SEM. As shown in Fig. 8, the iron hydroxide flocs were fluffier than the aluminum hydroxide flocs, which have big chunks. As mentioned, the aluminum hydroxide flocs have an open structure, and this kind of gel can potentially absorb more water than the iron hydroxide flocs.

## 4.5. MD performance

During membrane distillation, water vapor passes through the pores of a hydrophobic membrane. The membrane prevents direct transfer of water with dissolved solutes from the feed to the permeate side of the membrane. It is essential that dissolved organic compounds present in the feed be removed by EC. Fig. 5 indicates that the greatest reduction of TOC occurs when EC is conducted using a current of 5 A and 5 Al electrodes. Consequently water treated using these conditions was used for membrane distillation. As shown in Fig. 9A, during constant concentration operation, the normalized flux (normalized by dividing by the initial flux over the first 10 min of operation) for the produced water without EC pretreatment declined rapidly to 0.85 after 175 min of operation. Meanwhile the conductivity of the permeate increased to 35  $\mu$ S/cm, which indicates membrane fouling, pore wetting and salt passage. The normalized flux for the produced water pretreated by electrocoagulation using 5A for 5 min also decreased, though less than the

unpretreated water. Further the increase in the conductivity of the permeate is also much less. This shows that membrane fouling can be significantly mitigated by EC treatment. Foulants from the produced water, such as oil and grease, forming agents and surfactants [51] can be removed by EC treatment.

After 6 h of operation at constant concentration, 200 mL of the initial feed water was added to the feed tank and then the system run under concentration mode. The normalized flux vs. the operation time is shown in Fig. 9B. It is not unexpected that the normalized flux of these MD runs decrease with time. However, the rate of flux decrease is highest when non pretreated water is used. Again, the increase in conductivity is also less for EC pretreated water. The TSS and turbidity of the permeate after using MD for produced water treated at 5 min reaction time and 5A current is 0.8 mg  $\rm L^{-1}$  and 0.2 NTU, respectively.

The SEM images show changes in membrane morphology after use, unused membranes have open pores (shown in Fig. 10A and E). However, Fig. 10B and F shows blockage of the membrane pores if the unpretreated produced water is used. A brownish color can be observed on the membrane surface (shown in Fig. 11B). Instead of brown deposition from the un pretreated produced water, Fig. 11C shows white deposits on the membrane surface after the MD with EC treated produced water (5A with 5 min). This indicates that EC can effectively removes these brown color foulants, which is from the suspended organics and collides in the produced water [52]. There is much less deposition on the membrane surface if produced water is pretreated by EC as confirmed by SEM images (Fig. 10C and G).

The average elemental ratios of carbon/fluorine (C/F) and oxygen/fluorine (O/F) for all membranes before and after MD are given in Table 3. As can be seen the C/F and O/F ratios of all the membranes increased after MD, which is mainly due to organic fouling [25]. After MD, the C/F ratios of the membranes increased by 77.2 %, and 38.1 % compared to clean membrane, for the unpretreated produced water, and treatment with 5 min using 5A, respectively. As can be seen, the greatest increase in the C/F ratio was for the membrane challenged with unpretreated produced water due to the adsorption of the unremoved organic species. The membrane surface having the least organic foulants based on the C/F ratio change is for produced water pretreated using EC run.

Table 4 shows inorganic element atom percentages. The inorganic

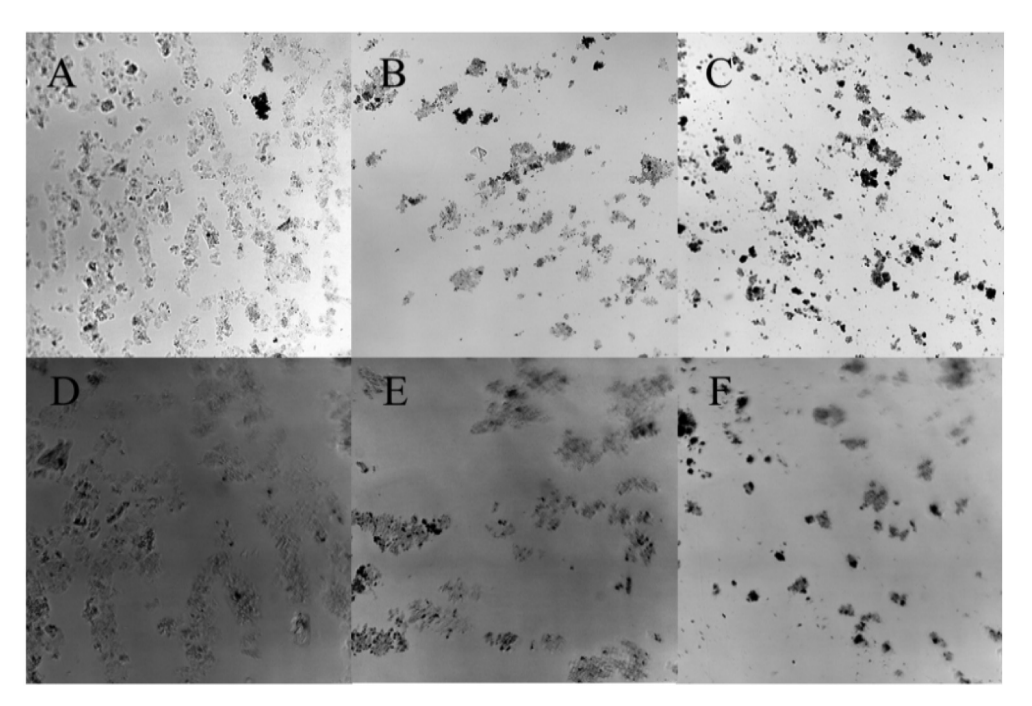


Fig. 7. LSCM images of sludge samples: 5A, 5 aluminum electrodes (A and D); 5A, 3 iron and 2 aluminum electrodes) (B and E); 5A, 5 iron electrodes (C and F).

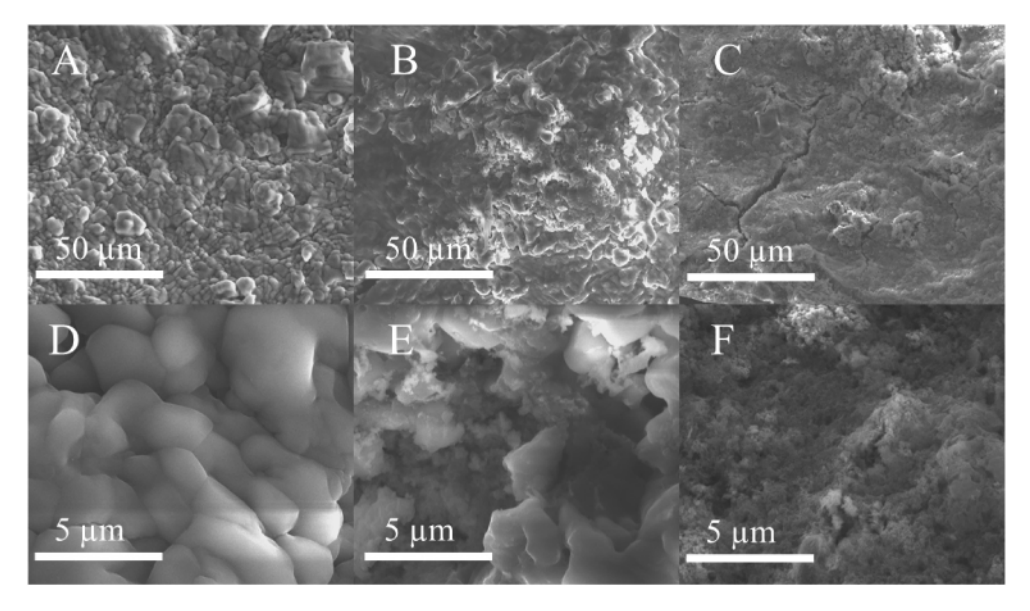


Fig. 8. SEM images of different sludge generated at 5 A current and 5 min reaction time using: (A and D) 5 aluminum electrodes; (B and E) 3 iron electrodes and 2 aluminum electrodes; (C and F) 5 iron electrodes.

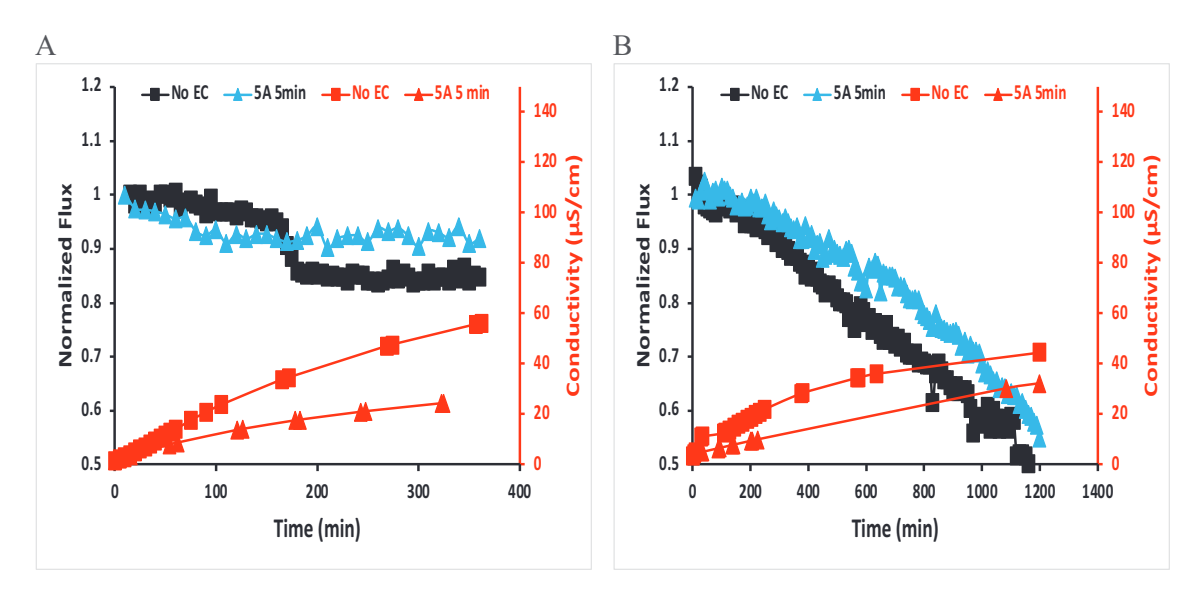


Fig. 9. Normalized flux and conductivity versus time for produced water streams: A) constant concentration mode; B) concentration mode. Note: No EC means unpretreated produced water; 5A 5 min means the feed water has been treated for 5 min using 5A.

foulants on the membrane could be strontium sulfate [53]. This is confirmed here since 7.65 % strontium was observed on the membrane surface for unpretreated produced water. Though strontium was not one of the major components in the produced water (see Table 2), this is probably due to relatively low solubility of strontium sulfate [53]. However, it seems EC can reduce strontium deposited on the membrane surface.

The results obtained here indicate that EC may be used as a pretreatment step prior to a unit operation like MD. Given the complexity of the EC process, determining suitable conditions for EC will be highly dependent on the feed water quality. The aim here was to maximize removal of TOC while ensuring that the floc settling characteristics were not adversely affected. However, the pretreatment goal will depend on the subsequent unit operation. It is important to determine the pretreatment conditions in conjunction with the subsequent unit operation.

## 5. Conclusions

Hydraulic fracturing produced water was treated by EC with Al electrodes, Fe electrodes, and Fe/Al electrodes. Sludge settling for EC conducted using Fe electrodes is much faster than the sludge generated by Al electrodes, which is likely due to the different morphology of metal hydroxides. The iron hydroxide particles were smaller and had a higher density. At higher current, Al hydroxides with gel-like structure were formed, which had lower settling speed because of the higher hydraulic resistances from the larger, lower density particles. The highest TOC removal efficiency of 42 % was obtained for EC with 5 Al electrodes at 5 A current and 5 min reaction time, which greatly decreased the membrane fouling during MD.

The results obtained here indicate that by considering the species present in the produced water the likely electrolysis reaction can be determined. However, EC is very complex as not only electrolysis reactions occur. Further successful EC will require effective flocculation

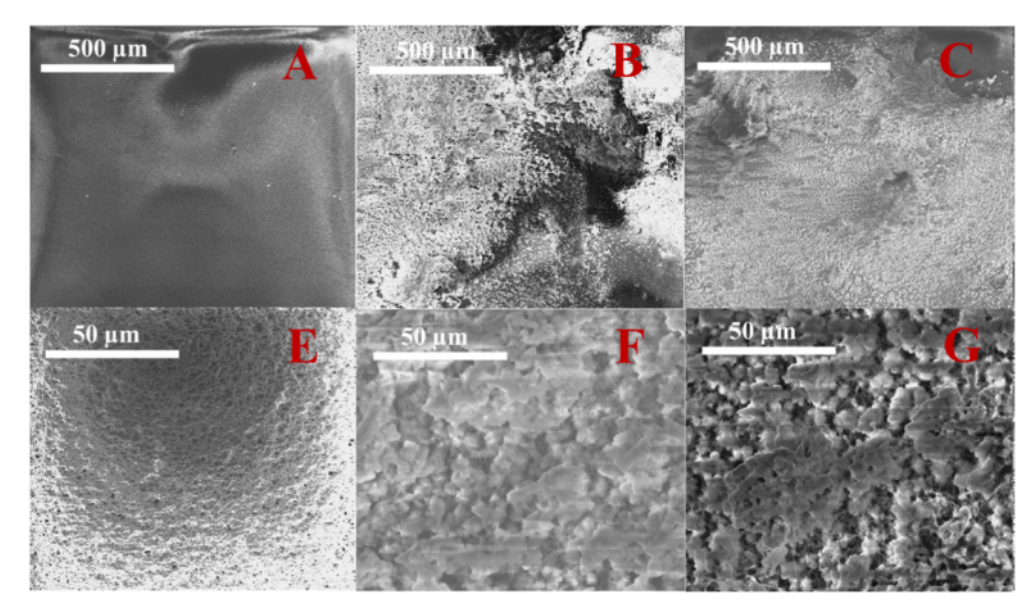
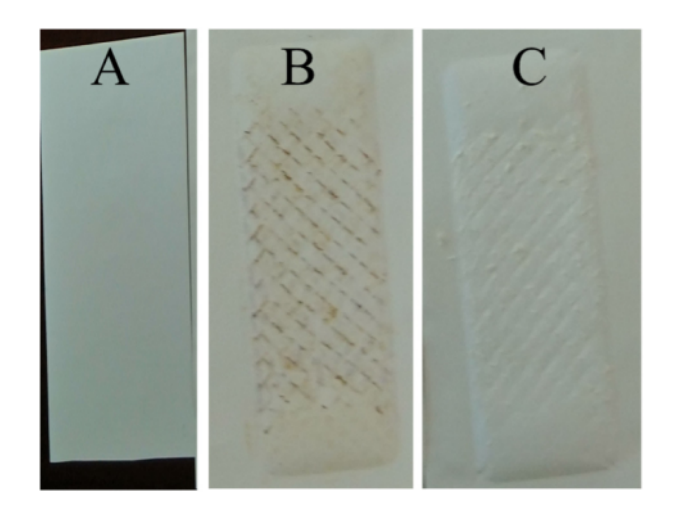


Fig. 10. SEM images of the membrane surface before and after MD: A and E are for virgin membrane; B and F are for MD with unpretreated produced water; C and G are for MD with 5 min EC using 5 A.



**Fig. 11.** Digital photos of membranes before and after MD using produced water: A) unused; B) unpretreated produced water; C) pretreated produced water with 5 A for 5 min residence time.

**Table 3**C/F and O/F atomic percent ratios for the membranes before and after MD.

MD feed condition	C/F atom percental ratio	O/F atom percental ratio
No MD run	3.02	0.40
Unpretreated produced water	5.35	6.33
5 A, 5 min treatment	4.17	6.17

and floc densification. These processes depend on the water quality and the operating conditions. By analyzing the floc properties, one can determine the removal efficiency of these species which can easily foul the membrane during MD. It is essential to design the EC and subsequent MD operations together in order to optimize the integrated process.

## **Funding**

Funding for this work was provided by the Arkansas Research

**Table 4** Element atom percentage of different membrane surfaces.

Elements	Atom percentage (%)			
	Clean membrane	Membrane after MD with unpretreated produced water	Membrane after MD run with EC treated produced water	
С	68.34	35.81	26.98	
0	8.96	42.33	39.89	
F	22.61	6.69	6.47	
Na	_	0.26	6.29	
S	_	6.47	5.99	
Cl	_	0.08	6.19	
Ca	_	0.52	0.80	
Sr	_	7.65	6.73	

Alliance, National Science Foundation through (a) Industry/University Cooperative Research Center for Membrane Science, Engineering and Technology, (IIP 1822101, 1913839, 1930079), (b) Research Experiences for Undergraduates REU Site: From Bench to Market: Engineering Systems for High Efficiency Separations (EEC 1659653) and the University of Arkansas. The authors gratefully acknowledge the financial support from the RAPID Manufacturing Institute, a public-private partnership between the Advanced Manufacturing Office (AMO) of the U.S. Department of Energy and the American Institute of Chemical Engineers (AIChE) under the subaward DE-EE0007888-08-08.

Funding for SRW was provided by a Research Fellowship Award No. FR-40-2020 from BARD, The United States-Israel Binational Agricultural Research and Development Fund.

## Declaration of competing interest

The authors declare the following financial interests/personal relationships which may be considered as potential competing interests:

S Ranil Wickramasinghe reports financial support was provided by The United States-Israel Binational Agricultural Research and Development Fund.

## Data availability

Data will be made available on request.

#### Acknowledgements

The author would like to acknowledge Ms. Alix Ineza Karangwa for his assistance with experiments.

## Appendix A. Supplementary data

Supplementary data to this article can be found online at https://doi.org/10.1016/j.jwpe.2022.103219.

#### References

- [1] X.(Cissy) Ma, X. Xue, A. González-Mejía, J. Garland, J. Cashdollar, Sustainable water systems for the city of tomorrow-a conceptual framework, Sustainability (Switzerland) 7 (2015) 12071–12105, https://doi.org/10.3390/su70912071.
- [2] E.H. Ezechi, M.H. Isa, S.R.M. Kutty, A. Yaqub, Boron removal from produced water using electrocoagulation, Process Saf. Environ. Prot. 92 (2014) 509–514, https:// doi.org/10.1016/j.psep.2014.08.003.
- [3] S. Jiménez, M.M. Micó, M. Arnaldos, F. Medina, S. Contreras, State of the art of produced water treatment, Chemosphere 192 (2018) 186–208, https://doi.org/ 10.1016/j.chemosphere.2017.10.139.
- [4] C.Onyems Igwe, A. al Saadi, Optimal options for treatment of produced water in offshore petroleum platforms, J. Pollut. Effects Control 01 (2013), https://doi.org/ 10.4172/2375-4397.1000102.
- [5] H. Huang, T. Babadagli, X. Chen, H. Li, Y. Zhang, Performance comparison of novel chemical agents for mitigating water-blocking problem in tight gas sandstones, in: SPE Reservoir Evaluation and Engineering, Society of Petroleum Engineers (SPE), 2020, pp. 1150–1158, https://doi.org/10.2118/199282-PA.
- [6] Q. Li, H. Xing, J. Liu, X. Liu, A review on hydraulic fracturing of unconventional reservoir, Petroleum. 1 (2015) 8–15, https://doi.org/10.1016/j. petlm.2015.03.008.
- [7] M.A. Reynolds, A technical playbook for chemicals and additives used in the hydraulic fracturing of shales, Energy Fuels 34 (2020) 15106–15125, https://doi. org/10.1021/acs.energyfuels.0c02527.
- [8] H. Huang, T. Babadagli, X. Chen, H. Li, Y. Zhang, Performance comparison of novel chemical agents for mitigating water-blocking problem in tight gas sandstones, in: SPE Reservoir Evaluation and Engineering, Society of Petroleum Engineers (SPE), 2020, pp. 1150–1158, https://doi.org/10.2118/199282-PA.
- [9] C.L. Conrad, T. Hanna, A.J. Atkinson, P.J.J. Alvarez, T.N. Tekavec, M.A. Reynolds, M.S. Wong, Y. ben Yin, Fit-for-purpose treatment goals for produced waters in shale oil andgasfields, Water Research. 173 (2020), https://doi.org/10.1016/j. watres.2020.115467.
- [10] B. al Hawli, A. Benamor, A.A. Hawari, A hybrid electro-coagulation/forward osmosis system for treatment of produced water, Chem. Eng. Process. Process Intensif. 143 (2019), https://doi.org/10.1016/j.cep.2019.107621.
- [11] A. Fakhru'l-Razi, A. Pendashteh, L.C. Abdullah, D.R.A. Biak, S.S. Madaeni, Z. Z. Abidin, Review of technologies for oil and gas produced water treatment, J. Hazardous Materials. 170 (2009) 530–551, https://doi.org/10.1016/j.ihazmat.2009.05.044.
- [12] A.M.A. Pintor, V.J.P. Vilar, C.M.S. Botelho, R.A.R. Boaventura, Oil and grease removal from wastewaters: Sorption treatment as analternative to state-of-the-art technologies. A critical review, Chem. Eng. J. 297 (2016) 229–255, https://doi. org/10.1016/j.cej.2016.03.121.
- [13] M.A. Al-Ghouti, M.A. Al-Kaabi, M.Y. Ashfaq, check <check>D.A. Da'na, Produced water characteristics, treatment and reuse: a review, J. Water Process Eng. 28 (2019) 222–239, https://doi.org/10.1016/j.jwpe.2019.02.001.
- [14] P. Sobolciak, A. Popelka, A. Tanvir, M.A. Al-Maadeed, S. Adham, I. Krupa, Materials and technologies for the tertiary treatment of produced water contaminated by oil impurities through nonfibrous deep-bed media: a review, Water (Switzerland) 12 (2020) 1–26, https://doi.org/10.3390/w12123419.
- [15] M. Jebur, S.R. Wickramasinghe, Hybrid membrane processes for treating oil and gas produced water, in: Integrated and Hybrid Process Technology for Water and Wastewater Treatment, Elsevier, 2021, pp. 339–369, https://doi.org/10.1016/ b978-0-12-823031-2.00019-7.
- [16] K.S. Hashim, A. Shaw, R. AlKhaddar, P. Kot, A. Al-Shamma'a, Water purification from metal ions in the presence of organic matter using electromagnetic radiationassisted treatment, Journal of Cleaner Production 280 (2021), https://doi.org/ 10.1016/j.iclepro.2020.124427.
- [17] B. Abdulhadi, P. Kot, K. Hashim, A. Shaw, M. Muradov, R. Al-Khaddar, Continuous-flow electrocoagulation (EC) process for iron removal from water: experimental, statistical and economic study, Sci. Total Environ. 760 (2021), https://doi.org/10.1016/j.scitotenv.2020.143417.
- [18] M.M. Emamjomeh, S. Kakavand, H.A. Jamali, S.M. Alizadeh, M. Safdari, S.E. S. Mousavi, K.S. Hashim, M. Mousazadeh, The treatment of printing and packaging wastewater by electrocoagulation–flotation: the simultaneous efficacy of critical parameters and economics, Desalin. Water Treat. 205 (2020) 161–174, https://doi.org/10.5004/dwt.2020.26339.
- [19] D.T. Moussa, M.H. El-Naas, M. Nasser, M.J. Al-Marri, A comprehensive review of electrocoagulation for water treatment: potentials and challenges, J. Environ. Manag. 186 (2017) 24–41, https://doi.org/10.1016/j.jenvman.2016.10.032.

- [20] M.Y.A. Mollah, P. Morkovsky, J.A.G. Gomes, M. Kesmez, J. Parga, D.L. Cocke, Fundamentals, present and future perspectives of electrocoagulation, J. Hazard. Mater. 114 (2004) 199–210, https://doi.org/10.1016/j.jhazmat.2004.08.009.
- [21] M. Yousuf, A. Mollah, R. Schennach, J.R. Parga, D.L. Cocke, Electrocoagulation (EC)-science and applications, J. Hazard. Mater. 84 (2001) 29–41, https://doi.org/ 10.1016/S0304-3894(01)00176-5.
- [22] Z. Al-Qodah, M. Al-Shannag, On the performance of free radicals combined electrocoagulation treatment processes, Sep. Purif. Rev. 48 (2019) 143–158, https://doi.org/10.1080/15422119.2018.1459700.
- [23] Z. Al-Qodah, Y. Al-Qudah, W. Omar, On the performance of electrocoagulationassisted biologicaltreatment processes: a review on the state of the art, Environ. Sci. Pollut. Res. 26 (2019) 28689–28713, https://doi.org/10.1007/s11356-019-06053-6
- [24] Z. Al-Qodah, Y. Al-Qudah, E. Assirey, Combined biological wastewater treatment with electrocoagulation as a post-polishing process: a review, Sep. Sci. Technol. (Philadelphia) 55 (2020) 2334–2352, https://doi.org/10.1080/ 01496395.2019.1626891.
- [25] M. Jebur, Y.H. Chiao, K. Thomas, T. Patra, Y. Cao, K. Lee, N. Gleason, X. Qian, Y. Hu, M. Malmali, S.R. Wickramasinghe, Combined electrocoagulation-microfiltration-membrane distillation for treatment of hydraulic fracturing produced water, Desalination 500 (2021), https://doi.org/10.1016/j.desal.2020.114886.
- [26] K. Sardari, P. Fyfe, S. Ranil Wickramasinghe, Integrated electrocoagulation forward osmosis – membrane distillation for sustainable water recovery from hydraulic fracturing produced water, J. Membr. Sci. 574 (2019) 325–337, https:// doi.org/10.1016/j.memsci.2018.12.075.
- [27] S.M.D.U. Islam, Electrocoagulation (EC) technology for wastewater treatment and pollutants removal, sustainable, Water Resour. Manag. 5 (2019) 359–380, https:// doi.org/10.1007/s40899-017-0152-1.
- [28] R. Chang, Chemistry, eighth, 2005.
- [29] J.N. Hakizimana, B. Gourich, M. Chafi, Y. Stiriba, C. Vial, P. Drogui, J. Naja, Electrocoagulation process in water treatment: a review of electrocoagulation modeling approaches, Desalination 404 (2017) 1–21, https://doi.org/10.1016/j. desal.2016.10.011.
- [30] G. Mouedhen, M. Feki, M.D.P. Wery, H.F. Ayedi, Behavior of aluminum electrodes in electrocoagulation process, J. Hazard. Mater. 150 (2008) 124–135, https://doi. org/10.1016/j.jhazmat.2007.04.090.
- [31] M. Kobya, O.T. Can, M. Bayramoglu, Treatment of textile wastewaters by electrocoagulation using iron and aluminum electrodes, J. Hazard. Mater. 100 (2003) 163–178, https://doi.org/10.1016/S0304-3894(03)00102-X.
- [32] P. Canizares, M. Carmona, J. Lobato, F. Martínez, M.A. Rodrigo, Electrodissolution of aluminum electrodes in electrocoagulation processes, Ind. Eng. Chem. Res. 44 (2005) 4178–4185, https://doi.org/10.1021/ie048858a.
- [33] G.K. Schweitzer, L.L. Pesterfield, The Aqueous Chemistry of the Elements, Oxford, 2010.
- [34] C. Barrera-Díaz, B. Bilyeu, G. Roa, L. Bernal-Martinez, Physicochemical aspects of electrocoagulation, Sep. Purif. Rev. 40 (2011) 1–24, https://doi.org/10.1080/ 15422119.2011.542737.
- [35] C. Barrera-Díaz, B. Bilyeu, G. Roa-Morales, P. Balderas-Hernández, A comparison of iron and aluminium electrodes in hydrogen peroxide-assisted electrocoagulation of organic pollutants, Environ. Eng. Sci. 25 (2008) 529–537, https://doi.org/ 10.1089/ees.2007.0106.
- [36] C.E. Barrera-Díaz, P. Balderas-Hernández, B. Bilyeu, Electrocoagulation: fundamentals and prospectives, in: Electrochemical Water and Wastewater Treatment, Elsevier, 2018, pp. 61–76, https://doi.org/10.1016/B978-0-12-813160-2.00003-1.
- [37] S. Zhao, G. Huang, G. Cheng, Y. Wang, H. Fu, Hardness, COD and turbidity removals from produced water by electrocoagulation pretreatment prior to reverse osmosis membranes, Desalination 344 (2014) 454–462, https://doi.org/10.1016/j. desal 2014 04 014
- [38] S. Garcia-Segura, M.M.S.G. Eiband, J.V. de Melo, C.A. Martínez-Huitle, Electrocoagulation and advanced electrocoagulation processes: a general review about the fundamentals, emerging applications and its association with other technologies, J. Electroanal. Chem. 801 (2017) 267–299, https://doi.org/10.1016/ j.jelechem.2017.07.047.
- [39] T.C. Timmes, H.C. Kim, B.A. Dempsey, Electrocoagulation pretreatment of seawater prior to ultrafiltration: pilot-scale applications for military water purification systems, Desalination 250 (2010) 6–13, https://doi.org/10.1016/j. desal.2009.03.021.
- [40] P. Cañizares, C. Jiménez, F. Martínez, C. Sáez, M.A. Rodrigo, Study of the electrocoagulation process using aluminum and iron electrodes, Ind. Eng. Chem. Res. 46 (2007) 6189–6195, https://doi.org/10.1021/ie070059f.
- [41] S. Zodi, O. Potier, F. Lapicque, J.P. Leclerc, Treatment of the textile wastewaters by electrocoagulation: effect of operating parameters on the sludge settling characteristics, Sep. Purif. Technol. 69 (2009) 29–36, https://doi.org/10.1016/j. seppur.2009.06.028.
- [42] R. Font, P. García, M. Rodriguez, Sedimentation test of metal hydroxides: hydrodynamics and influence of pH, Colloids Surf. A Physicochem. Eng. Asp. 157 (1999) 73–84, https://doi.org/10.1016/S0927-7757(99)00091-6.
- [43] R.I. Dick, K. Young, Analysis of thickening performance of final settling tanks, in: Proceedings of the 27th Industrial Waste Conference, 1972, p. 33.
- [44] T.D. Reynolds, P.A.C. Richards, Unit Operations and Processes in Environmental Engineering, PWS Publishing Company, 1995.
- [45] L.C. Hua, C. Huang, Y.C. Su, T.N.P. Nguyen, P.C. Chen, Effects of electrocoagulation on fouling mitigation and sludge characteristics in a coagulation-

- assisted membrane bioreactor, J. Membr. Sci. 495 (2015) 29–36, https://doi.org/10.1016/j.memsci.2015.07.062.
- [46] B. Jin, B.M. Wilén, P. Lant, A comprehensive insight into floc characteristics and their impact on compressibility and settleability of activated sludge, Chem. Eng. J. 95 (2003) 221–234, https://doi.org/10.1016/S1385-8947(03)00108-6.
- [47] K.P. Papadopoulos, R. Argyriou, C.N. Economou, N. Charalampous, S. Dailianis, T. I. Tatoulis, A.G. Tekerlekopoulou, D.v. Vayenas, Treatment of printing ink wastewater using electrocoagulation, Journal of Environmental Management. 237 (2019) 442–448, https://doi.org/10.1016/j.jenvman.2019.02.080.
- [48] B.M.B. Ensano, L. Borea, V. Naddeo, V. Belgiorno, M.D.G. de Luna, F.C. Ballesteros, Removal of pharmaceuticals from wastewater by intermittent electrocoagulation, Water (Switzerland) 9 (2017), https://doi.org/10.3390/w9020085.
- [49] D. Kartikaningsih, Y.J. Shih, Y.H. Huang, Boron removal from boric acid wastewater by electrocoagulation using aluminum as sacrificial anode, Sustain. Environ. Res. 26 (2016) 150–155, https://doi.org/10.1016/j.serj.2015.10.004.
- [50] A.S. Fajardo, R.F. Rodrigues, R.C. Martins, L.M. Castro, R.M. Quinta-Ferreira, Phenolic wastewaters treatment by electrocoagulation process using Zn anode, Chem. Eng. J. 275 (2015) 331–341, https://doi.org/10.1016/j.cej.2015.03.116.
- [51] Y.H. Chiao, M.B.M.Y. Ang, Y.X. Huang, S.S. Depaz, Y. Chang, J. Almodovar, S. R. Wickramasinghe, A "graft to" electrospun zwitterionic bilayer membrane for the separation of hydraulic fracturing-produced water via membrane distillation, Membranes (Basel) 10 (2020) 1–14, https://doi.org/10.3390/membranes10120402.
- [52] A.K. Thakur, I.M. Hsieh, M.R. Islam, B. Lin, C.C. Chen, M. Malmali, Performance of sweeping gas membrane distillation for treating produced water: modeling and experiments, Desalination 492 (2020), https://doi.org/10.1016/j. desal.2020.114597.
- [53] I.M. Hsieh, A.K. Thakur, M. Malmali, Comparative analysis of various pretreatments to mitigate fouling and scaling in membrane distillation, Desalination 509 (2021), https://doi.org/10.1016/j.desal.2021.115046.